X-ray diffraction study of alternating nanocrystalline silicon/amorphous silicon multilayers

X. L. Wu,[a] S. Tong, X. N. Liu, X. M. Bao, S. S. Jiang, and D. Feng
National Laboratory of Solid State Microstructures and Department of Physics, Nanjing University, Nanjing 210093, People's Republic of China

G. G. Siu
Department of Physics and Materials Science, City University of Hong Kong, Kowloon, Hong Kong

(Received 26 July 1996; accepted for publication 9 December 1996)

Structural properties of alternating nanocrystalline silicon/amorphous silicon multilayers with visible light emission at room temperature were examined by means of x-ray diffraction. According to the linewidths and intensities of the diffraction peaks in the low- and high-angle ranges, we have determined the effective interface thickness, the mean crystallite sizes, and the internal strains, which are closely related to the photoluminescence in this material. In addition, the existence of the voids or holes was also observed, indicating that the improved electrical properties of this kind of hydrogenated nanocrystalline materials are due to the inhomogeneous structure of the material. © *1997 American Institute of Physics.* [S0003-6951(97)01707-5]

Structural properties of Si-based materials with visible emission have motivated a great deal of experimental and theoretical research effort.[1–5] Recently, we reported observation of the stable photoluminescence (PL) in layer-by-layer deposited hydrogenated nanocrystalline Si/amorphous Si (nc-Si:H/α-Si:H) multilayers (MLs).[6,7] For a MLs sample with a single sublayer thickness of just a few crystal lattice constants, deviations from perfect periodicity, caused by layer thickness fluctuations along the growth direction, interfacial roughness, and interfacial broadening due to material intermixing, will have large influence on the PL. In this letter, we investigated the structural properties of this kind of PECVD material by means of x-ray diffraction technique on the basis of the previous work.[6,7] The mean crystallite sizes and effective interface thickness were calculated. The internal strain was estimated and results were compared with those from the Raman scattering.

Polished crystal Si wafers with (100) orientation, p-type and 1–3 Ω cm resistivity were used as substrates. MLs samples were deposited with a conventional diode glow discharge system with capacitance electrodes. During sample deposition, the substrate temperature was controlled at 300 °C and the rf power density of the glow discharge at 0.44 W/cm^2. The rf source was interrupted at each step of individual layer deposition to keep the interfaces abrupt. Two MLs samples (A and B) were prepared with 50 repeat periods each. The thickness of single nc-Si:H and α-Si:H sublayers in sample A are 3 and 8 nm, respectively, and those in sample B are 2.2 and 8 nm each. Details of sample preparation have bene described in the previous literature.[6,8] X-ray diffraction (XRD) experiments were carried out on a Rigaku 3015 type single crystal diffractometer using Cu Kα radiation. Data were collected in the range 2θ=1.0 to 50° and the corresponding background scattering was subtracted. The wavelength of x ray is 0.154 nm.

Figures 1 and 2 show x-ray diffraction patterns of samples A and B in the low angle range 2θ=1 to 5°. Reflexes of m up to 4 are observed (the first-order reflex is missed due to limited experimental conditions), giving direct evidence for the one-dimensional periodicity. Comparing the linewidths of the same reflective orders between samples A and B, it can be seen that sample A has smaller full-widths at half-maximum (FWHM) and more inhomogeneous distributions of the diffraction peaks than sample B, indicating that sample A has larger fluctuation in the thickness of the individual periods than sample B. In addition, from Fig. 1, we can observe a broad peak at around 2θ=3.5°. The structure is closely related to a distribution of voids or holes containing an undetermined amount of hydrogen (x rays are only weakly scattered by the hydrogen relative to the Si atoms) similar to that found in evaporated α-Si:H samples.[9,10] To corroborate this result and obtain the mean crystallite sizes, high angle XRD measurements were also carried out for the 2θ range of 5–50°. The obtained experimental results are shown in Figs. 3(a) and 3(b) for samples A and B, respectively. These figures clearly show a broad peak structure at about 2θ=13° in addition to a broadened (111) peak, indicating that the samples contain the existence of the voids or holes.[10] According to their relative intensities, we can infer that sample A has a larger inhomogeneity than sample B.

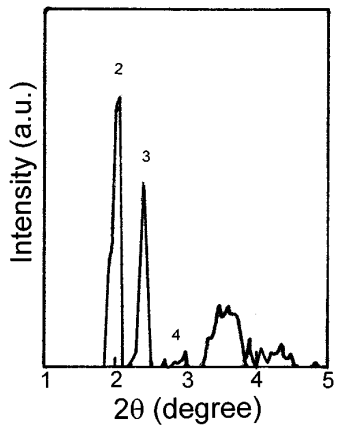

FIG. 1. Low-angle θ–2θ x-ray diffraction pattern of sample A. The labeled numbers indicate the reflection orders. A broad peak from material inhomogeneity can be seen at about 2θ=3.5°.

[a]Electronic mail: xmbao@nju.edu.cn or postphys@nju.edu.cn

 0003-6951/97/70(7)/838/3/$10.00 © 1997 American Institute of Physics
Downloaded¬19¬Sep¬2009¬to¬131.188.168.55.¬Redistribution¬subject¬to¬AIP¬license¬or¬copyright;¬see¬http://apl.aip.org/apl/copyright.jsp

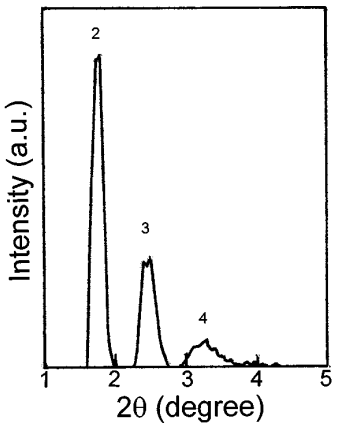

FIG. 2. Low-angle θ–2θ x-ray diffraction pattern of sample B. The labeled numbers indicate the reflection orders.

Thus, the improved electrical properties[11] of this material are not the result of the material being free from microregions of low electron density. The visible PL may be in part connected with the inhomogeneity.

From the low angle XRD results obtained above, we can calculate the repetition period and the effective interfacial thickness. The low-angle XRD region is due to scattering from the chemical modulation of the layers. The peak positions are given by[12]

$$\sin^2\theta = (m\lambda/2d)^2 + 2\delta, \tag{1}$$

where θ is the angle of the peak position, m is the order of the reflection, λ is the x-ray wavelength, and δ is the real part of the multilayer's average index of reflection. The correction to Bragg's law in the previous equation is significant for 2θ values less than three degrees, since δ is typically of the order 10^{-5}.[13] From the superlattice reflection orders of $m=2$ and 3 from sample A, the repetition periods were calculated to be 91 ± 1 and 113 ± 1 Å, respectively. The result from $m=2$ is not consistent with the nominal value of 110 Å determined from the deposition conditions, also indicating that this material does not have a good periodicity. The thickness of the individual periods has a large fluctuation. For sample B, the repetition periods from $m=2$ and 3 superlattice peaks were calculated to be 104 ± 1 and 109 ± 1 Å, in good agreement with the nominal value of 102 Å from deposition conditions.

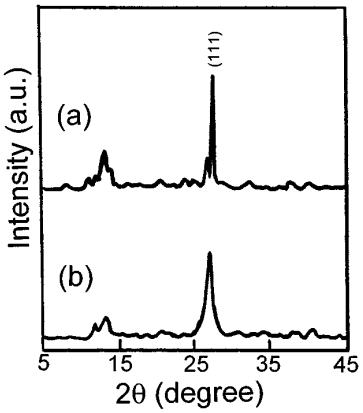

FIG. 3. High-angle θ–2θ x-ray diffraction patterns of (a) sample A and (b) sample B. The appearance of the peak at $2\theta=13°$ shows the existence of the voids or holes in the samples.

The interfacial structure has a large influence on the PL efficiency. According to the intensities of different Bragg reflection orders in the low angle range, we can calculate this effective interface thickness. In the absence of resonance effects, the intensity of the mth order reflex is proportional to[14,15]

$$I_{x,m} \sim K \tan\theta_{x,m} \sin\theta_{x,m} |F_{x,m}|^2/m^3, \tag{2}$$

where $\theta_{x,m}$ is the incidence angle of the mth reflex. K is a factor which accounts for the polarization of the incident beam and takes the value $(1+|\cos 2\theta_{x,m}|)/2$ for unpolarized radiation. The factor $F_{x,m}$ is the mth Fourier component of the electronic density profile. This factor is determined by the relative thickness of the layers and by the width and composition profile of the interfaces. If we assume a Gaussian error profile for the variation in composition across and interface, the square of the mth Fourier transform can be given by[15]

$$F_{x,m}^2 = [4\sin^2(m\pi d_1/d)/m^2\pi^4]\exp[-(2m\pi\sigma_m/d)^2]R_m. \tag{3}$$

Here $d=d_1+d_2$ is the modulation wavelength of a MLs. d_1 is the thickness of single nc-Si:H sublayer. σ_m is the characteristic half-width of the interface due to intermixing effects. The sinusoidal term is a structural factor for an ideal two-layer MLs with abrupt interfaces. The factor R_m reflects deviations from perfect periodicity caused by layer thickness fluctuations along the grown direction and by interface roughness. Such deviations induce incoherent scattering thereby reducing the intensity of the scattered peaks. If these fluctuations are completely random and their amplitude small compared to the nominal layer thicknesses, R_m is given by a Debye–Waller-like factor[14,16] and thus the intensity I_m of the x-ray diffraction peak can be stated as

$$I_m \sim [\sin^2(m\pi d_1/d)/m^2]\exp[-(2\pi m\sigma/d)^2], \tag{4}$$

where σ is an effective interface half-width that takes into account material intermixing, interface roughness, and layer thickness fluctuation. Within the limitations of the present model, each of the effects contributes in the same way to the effective interface thickness $d_e=2\sigma$. Note that Eq. (4) does not include the effect from material inhomogeneities such as the voids or holes etc. Therefore, the real interface thickness will be larger than that calculated from Eq. (4), since the material inhomogeneities are to increase the interface roughness.

To calculate the effective thickness, we measured the integrated intensities of the reflection orders $m=2$ and 3 from samples A and B. These integrated intensities depend not only on the modulation profile but also on the optical absorption coefficient and the total thickness of the samples. To correct these differences when comparing different samples, the obtained integrated intensities were normalized to the scattering intensity of $2\theta\approx28°$ peak in the high-angle region and denoted by I_n. Using Eq. (4), we can calculate the slope from the dependence of the quantity $\ln[I_n/\sin^2(\pi d_1/d)]$ vs $(2\pi/d)^2$ and therefore obtain the effec-

Downloaded¬19¬Sep¬2009¬to¬131.188.168.55.¬Redistribution¬subject¬to¬AIP¬license¬or¬copyright;¬see¬http://apl.aip.org/apl/copyright.jsp

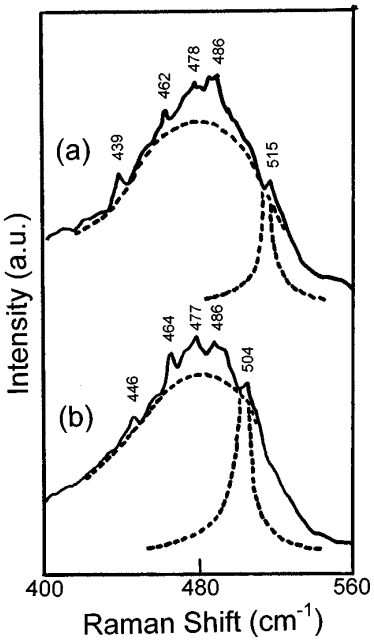

FIG. 4. Raman spectra of (a) sample *A* and (b) sample *B* in the frequency range of 400–560 cm^{-1}. Four small peaks superposed on the broad peak of α-Si:H at 480 cm^{-1}can be clearly observed.

tive interface thickness to be 16 and 12 Å for samples *A* and *B*, respectively. This result indicates that sample *B* has a sharper interface between *nc*-Si:H and α-Si:H sublayers and therefore stronger PL intensity than sample *A*.[7]

According to the result obtained from Fig. 3, we can calculate the mean crystallite sizes in our MLs samples. According to Scherrer's formula,[17] the mean sizes of nanocrystallites depend on the half-width of the (111) diffraction peak and are found to be 2.8 and 1.9 nm for samples *A* and *B*, respectively. These values are basically in agreement with those from Raman scattering (3.5 and 2.2 nm for samples *A* and *B*).[18] The small difference between the Raman scattering and x-ray diffraction may arise from the material inhomogeneities such as the voids, holes, internal strain, etc.

Next, we give an analysis for the internal strain. The existence of the internal strains has been confirmed in the previous Raman scattering results.[18] Now we estimate their magnitudes according to x-ray diffraction results. In Fig. 3, the diffraction angle of the (111) plane was shifted toward the low-angle side from $2\theta=28.47°$ for single crystal to 27.11 (sample *A*) and 26.94° (sample *B*). The calculated spacings of the (111) planes are 3.29 (sample *A*) and 3.31 Å (sample *B*). The elastic tensile strain *S* can be calculated approximately by[19]

$$S=(a-a_0)/a_0, \tag{5}$$

where a_0 is the lattice constant of single-crystal Si and a is the measured lattice constant of the samples due to the internal strain. The strain values obtained from Eq. (5) are found to be 4.8% and 5.4% for samples *A* and *B*, respectively. To confirm the result, we estimate the strain values from the Raman scattering results. Figures 4(a) and 4(b) show the Raman spectra of samples *A* and *B* in the frequency range of 400–560 cm^{-1}, respectively. Using the following formula, we can calculate the elastic tensile strains *s*

$$(\omega_c-\omega_s)/\omega_c=-s(P+2Q)/2\omega_c^2, \tag{6}$$

where $P=-1.43\ \omega_c^2$ and $Q=-1.89\omega_c^2$ are the phonon deformation potentials of silicon. ω_c is the frequency of the crystalline peak. ω_s is the vibrational frequency of the shell region between the crystalline core and the outer space in nanocrystallites.[18,20] From Fig. 4, it can be seen that the band ω_s consists of four small peaks and therefore four strain values can be obtained from Eq. (6). We take the average value of four strains as the effective strain. The effective strains are found to be about 5.7% and 4.4% for samples *A* and *B*, in good agreement with the values obtained from the lattice expansion. This result indicates that the inhomogeneity of sample *A* does not mainly come from the internal strain. It may be related to the voids or holes.

In conclusion, we have presented experimental results on the interfacial structure, the mean crystallite sizes, the internal strain distribution and the material inhomogeneities in the alternating *nc*-Si:H/α-Si:H MLs by analyzing the intensities and linewidths of x-ray diffraction peaks in the low and high angle ranges. The obtained results are compared with those from Raman scattering and good agreement is achieved.

[1] L. T. Canham, Appl. Phys. Lett. **57**, 1046 (1990).
[2] L. S. Liao, X. M. Bao, Z. F. Yang, and N. B. Min, Appl. Phys. Lett. **66**, 2382 (1995).
[3] D. Ruter, T. Kunze, and W. Bauhofer, Appl. Phys. Lett. **64**, 3006 (1994).
[4] M. K. Lee and K. R. Peng, Appl. Phys. Lett. **62**, 3159 (1993).
[5] X. L. Wu, F. Yan, X. M. Bao, N. S. Li, L. S. Liao, M. S. Zhang, S. S. Jiang, and D. Feng, Appl. Phys. Lett. **68**, 2091 (1996).
[6] S. Tong, X. N. Liu, and X. M. Bao, Appl. Phys. Lett. **66**, 469 (1995).
[7] X. L. Wu, G. G. Siu, S. Tong, F. Yan, S. S. Jiang, X. K. Zhang, and D. Feng (unpublished).
[8] X. N. Liu, X. W. Wu, X. M. Bao, and Y. L. He, Appl. Phys. Lett. **64**, 220 (1994).
[9] N. J. Shevchik and W. Paul, J. Non-Cryst. Solids **16**, 55 (1974).
[10] P. D'Antonio and J. H. Konnert, Phys. Rev. Lett. **43**, 1161 (1979).
[11] Y. L. He, C. Z. Yin, G. X. Cheng, L. C. Wang, and X. N. Liu, J. Appl. Phys. **75**, 797 (1994).
[12] P. F. Miceli, D. A. Neumann, and H. Zabel, Appl. Phys. Lett. **48**, 24 (1986).
[13] E. E. Fullerton, I. K. Schuller, H. Banderstraeten, and Y. Bruynseraede, Phys. Rev. B **45**, 9292 (1992).
[14] B. Abeles, T. Tiedje, K. S. Liang, H. W. Deckman, H. C. Stasiewski, J. C. Scanlar, and P. M. Eisenberger, J. Non-Cryst. Solids **66**, 351 (1984).
[15] P. V. Santos, M. Hundhausen, L. Ley, and C. Viczian, J. Appl. Phys. **69**, 778 (1991).
[16] N. W. Ashcroft and N. D. Mermin, *Solid State Physics* (Hold, Rinehart, and Winston, Philadelphia, 1981), p. 790.
[17] Scherrer, Proc. Phys. Soc. London, Sec. A **62**, 741 (1949).
[18] X. L. Wu, G. G. Siu, S. Tong, F. Yan, S. S. Jiang, X. K. Zhang, and D. Feng, Appl. Phys. Lett. **69**, 523 (1996).
[19] H. Xia, Y. L. He, L. C. Wang, W. Zhang, X. N. Liu, X. K. Zhang, and D. Feng, J. Appl. Phys. **78**, 6705 (1995).
[20] Y. Kanemitsu, T. Ogawa, K. Shirashi, and K. Takeda, Phys. Rev. B **48**, 4883 (1993).

Downloaded¬19¬Sep¬2009¬to¬131.188.168.55.¬Redistribution¬subject¬to¬AIP¬license¬or¬copyright;¬see¬http://apl.aip.org/apl/copyright.jsp